Research Article

The Synthesis of NiO/TiO$_2$ Heterostructures and Their Valence Band Offset Determination

Z. H. Ibupoto,[1] M. A. Abbasi,[1] X. Liu,[2] M. S. AlSalhi,[3,4] and M. Willander[1]

[1] *Physical Electronics and Nanotechnology Division, Department of Science and Technology, Campus Norrköping, Linköping University, 60174 Norrköping, Sweden*
[2] *Department of Physics, Chemistry & Biology (IFM), Linköping University, 58183 Linköping, Sweden*
[3] *Physics and Astronomy Department, College of Science, King Saud University, P.O. Box 2455, Riyadh 11451, Saudi Arabia*
[4] *Research Chair for Laser Diagnosis of Cancer, King Saud University, P.O. Box 2455, Riyadh 11451, Saudi Arabia*

Correspondence should be addressed to Z. H. Ibupoto; zafar.hussain.ibupoto@liu.se

In this work, a heterojunction based on p-type NiO/n-type TiO$_2$ nanostructures has been prepared on the fluorine doped tin oxide (FTO) glass substrate by hydrothermal method. Scanning electron microscopy (SEM) and X-Ray diffraction techniques were used for the morphological and crystalline arrays characterization. The X-ray photoelectron spectroscopy was employed to determine the valence-band offset (VBO) of the NiO/TiO$_2$ heterojunction prepared on FTO glass substrate. The core levels of Ni 2p and Ti 2p were utilized to align the valence-band offset of p-type NiO/n-type TiO$_2$ heterojunction. The valence band offset was found to be ~0.41 eV and the conduction band was calculated about ~0.91 eV. The ratio of conduction band offset and the valence-band offset was found to be 2.21.

1. Introduction

Recently, the fabrication and the engineering of nanostructures based on metal oxides have drawn effective attention of the researchers due to their specific electronic and optoelectronic features and more practical applications in the industry and technology [1]. Among the various metal oxides, the nanostructures of titanium dioxide (TiO$_2$) are more popular because of their uniqueness and attractive properties in optics, electronics, photochemistry, and biology in addition to its usability in the fabrication of photovoltaic devices [2–4], lithium ion batteries [5], dye-sensitized solar cells [6, 7], and photocatalysts [8–15]. Different methods have been used to enhance the photocatalysts properties of titanium dioxide such as TiO$_2$-carbon hybrids and doping of TiO$_2$ with metals and nonmetals has also significant contribution on the photocatalysts properties of titanium dioxide nanomaterial [10–12].

Several growth techniques have been used for the synthesis of one dimensional TiO$_2$ nanostructures such as hydrothermal [16], template synthesis [17, 18], electrochemical etching [19, 20], chemical vapor deposition [21], and sol-gel process [22, 23]. Among above mentioned methods, the hydrothermal technique is highly promising because of its low temperature, simple, cost effectiveness, and the environment friendly advantages.

Besides titanium dioxide, nickel oxide (NiO) is p-type semiconductor material and is widely used in different applications such as transparent conductive films [24], electrochromic devices [25], as a potential candidate in the chemical sensors [26, 27]. NiO exhibits a wide bandgap of 3.6–4.0 eV at room temperature; thus, NiO is considered transparent in the visible light region. Moreover, NiO is largely used as a cocatalyst with different n-type semiconductors due its high p-type concentration, high hole mobility, and low cost [28]. The existence of NiO enhances the separation of electron and hole pairs via electric junction field and also promotes the interfacial charge transfer [29–31]. NiO nanostructures can be synthesized by sputtering [32], chemical vapor deposition [33, 34], hydrothermal method [27], and the sol-gel method
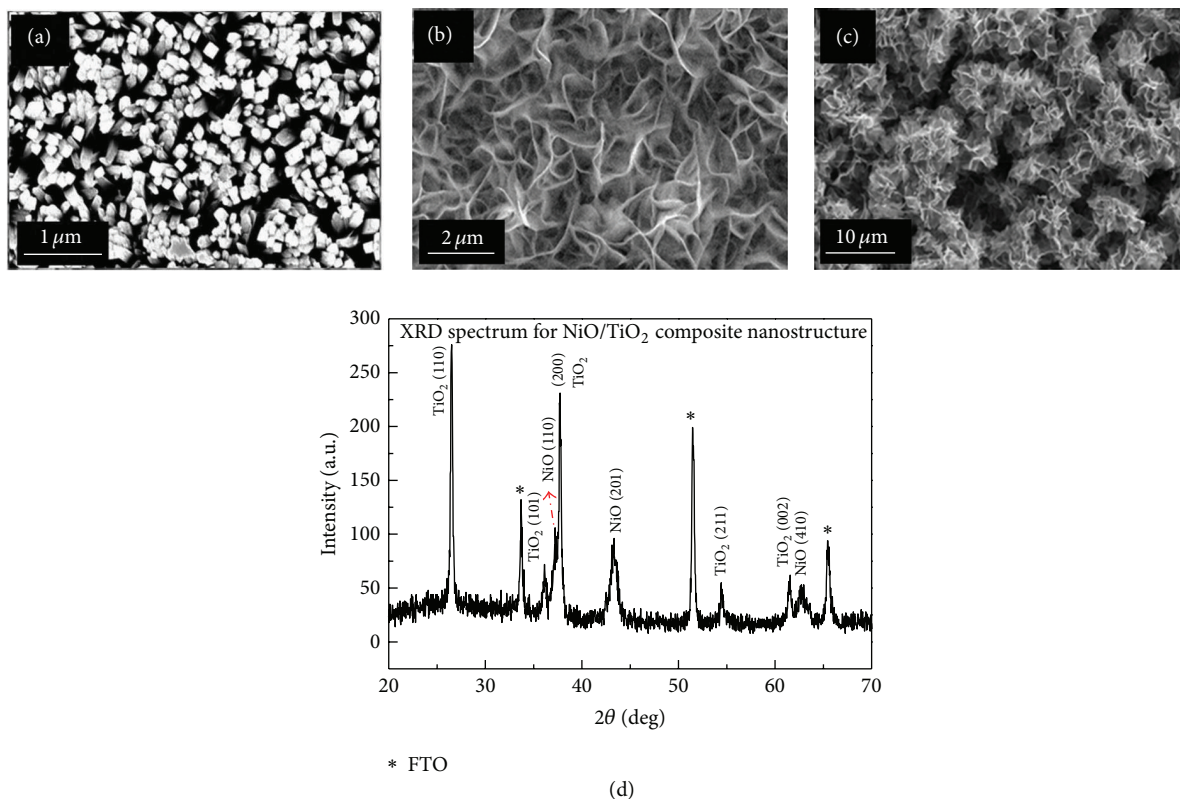
FIGURE 1: (a) The SEM image of pure TiO_2 nanorods, (b) SEM image of pure NiO nanostructures, (c) SEM image of heterostructures of p-type NiO/n-type TiO_2 nanostructures, and (d) XRD of the composite nanostructures.

[35, 36]. The hydrothermal method for the synthesis of NiO nanostructures is relatively more favourable due to its benign features and simplicity.

After surveying the literature it is known that the valence-band offset (VBO) of NiO/ZnO heterojunction has been investigated by few researchers. The growth pattern in their research was as follows: in some cases NiO was used as substrate and ZnO as the epitaxial layer [37, 38]. However in several cases NiO/ZnO based light emitting diodes, ZnO was used as substrate and NiO as the epitaxial layer [39]. The valence-band offset of many heterojunctions determined by XPS is closely linked to the process of growth of heterostructures [40]. To date there is no report about the determination of valence-band offset of NiO/TiO_2 heterostructures.

In the present work, the fabrication and the design of TiO_2 and NiO heterostructures are followed by hydrothermal method. Moreover, the valence-band offset (VBO) of NiO/TiO_2 heterojunction is measured by XPS technique. The structural characterization of fabricated heterostructures was determined by scanning electron microscopy (SEM) and X-ray diffraction (XRD) techniques.

2. Experimental Section

The growth process of the presented p-n junction based on TiO_2 and NiO nanostructures on the fluorine doped tin oxide (FTO) glass substrate by hydrothermal method

was as follows. Firstly, a commercially available and cleaned FTO substrate was used for the synthesis of TiO_2 and NiO nanostructures. In a typical process 1 mL of TTIP, 20 mL of 37% hydrochloric acid, and 40 mL of deionized water were mixed at constant stirring for 30 minutes. The growth solution was transferred into Teflon vessel of 125 mL capacity and it was sealed in autoclave and kept in preheated oven at 110°C for 12 hours. Afterwards, the TiO_2 nanostructures grown FTO substrate was washed with the deionized water and dried at room temperature. NiO nanostructures were grown on the TiO_2 nanostructures by hydrothermal method using equimolar concentration of (0.1M) nickel chloride hexahydrate and hexamethylenetetramine and the growth solution was letf at 95°C for 4-6 hours in preheated electric oven. After the completion of growth time, the heterostructures were washed with the deionized water and dried with the flow of nitrogen gas at room temperature. Then heterostructures were annealed at 450°C for the complete conversion of Ni(OH)$_2$ nanostructures into NiO crystalline phase. The structural characterization was performed by scanning electron microscopy and X-ray diffraction and the core levels and valence-band (VB) spectra of the prepared sample were measured by X-ray photoelectron spectrometer (XPS, Thermo ESCALAB 250) using a 1486.6 eV Al Kα source. All XPS spectra were measured by the C 1s peak (284.8 eV) as a reference substance in order to compensate the charge effect.
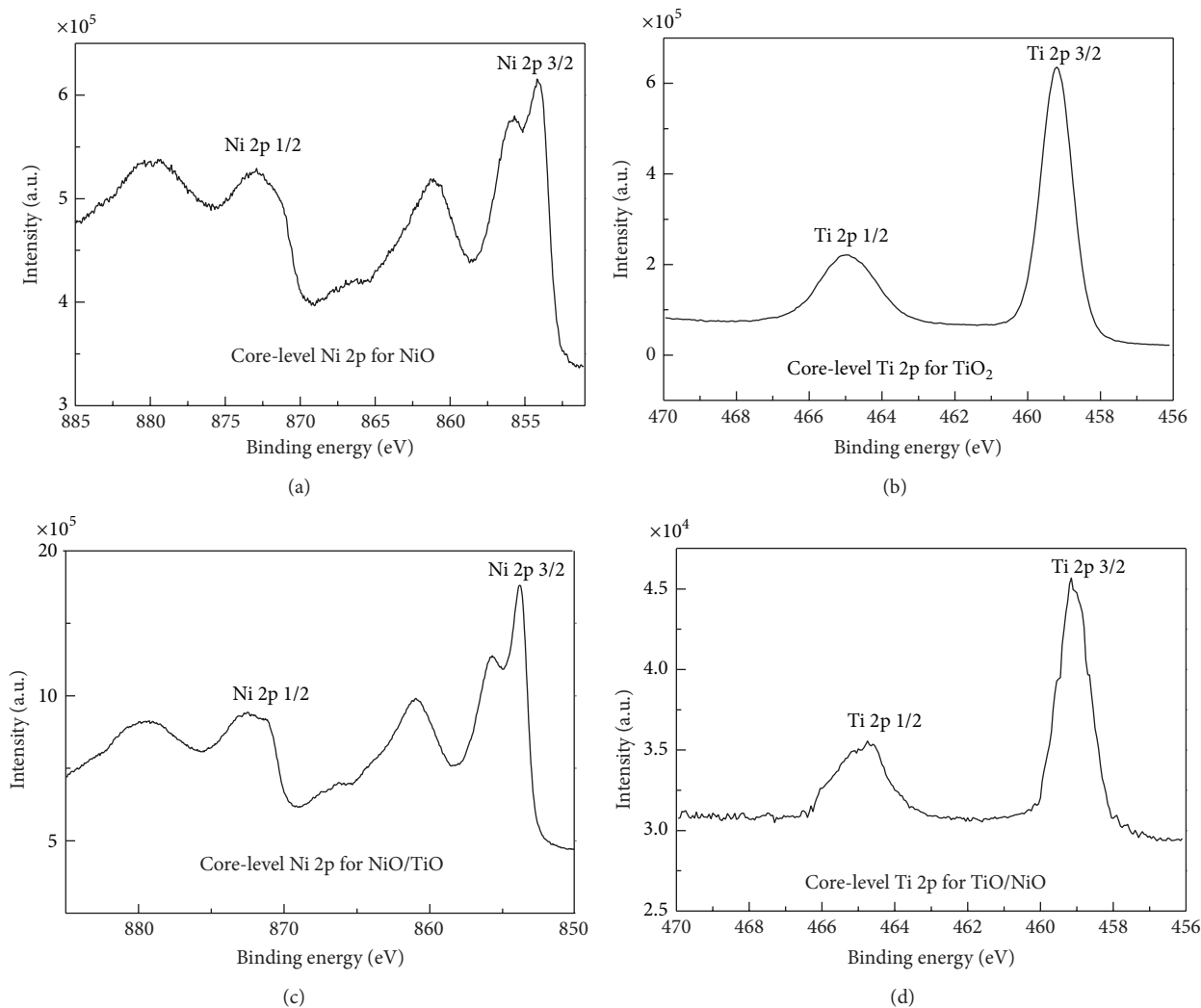
FIGURE 2: The XPS measurement for the calculation of valence-band offset of the developed heterojunction of p-type NiO/n-type TiO$_2$ nanostructures, (a) Ni 2p spectrum of pure NiO, (b) Ti 2p spectrum of pure TiO$_2$, (c) Ni 2p spectrum of heterostructures, and (d) Ti 2p spectrum of heterostructures.

3. Results and Discussion

3.1. The Structural Characterization of p-Type NiO/n-Type TiO$_2$ Heterostructures.
A typical SEM image of TiO$_2$ nanostructures grown on FTO glass substrate by hydrothermal growth technique is shown in Figure 1(a). It can be seen that nanostructures are dense and perpendicular to the substrate. The average diameter and length of nanostructures are 100 nm and 500 nm, respectively. Figure 1(b) shows the SEM image of NiO nanostructures and it can be observed that the nanostructures are like a porous structure. Figure 1(c) shows the composite structures of NiO/TiO$_2$ nanostructures and from the presented image it is clear that almost top surface of TiO$_2$ nanostructures is fully covered with the nanostructures of NiO.

Figure 1(d) shows the diffraction pattern of NiO/TiO$_2$ nanostructures grown on the FTO glass substrate at room temperature. All the diffraction peaks could be assigned to

rutile phase of TiO$_2$ and well match to the JCPDS (card number 211276). The intense (002) peak reflects that the preferred orientation of TiO$_2$ nanorods is along the (001) direction. However, some peaks of NiO are also shown in Figure 1(d) and it can be seen that the sample is composed of NiO and TiO$_2$ nanostructures. Some diffraction peaks also appeared for FTO glass substrates which are indicated by star sign.

3.2. The Calculation of Band Offset by XPS Measurement.
Figure 2 shows the core level (CL) spectrum of spin-orbit splitting of Ti 2p and Ni 2p peaks. The CL spectrum of Ni 2p 3/2 is represented by Figure 2(a) and two dominant peaks are found at 854.13 eV and 855.78 eV which are mainly concerned the Ni–O linkages. Figure 2(b) shows that the Ti 2p 3/2 peak at 458.3 ± 0.1 eV is indexed to the Ti–O bond and the peak at 464.0±0.1 eV is assigned to the Ti 2p 1/2 oxidation
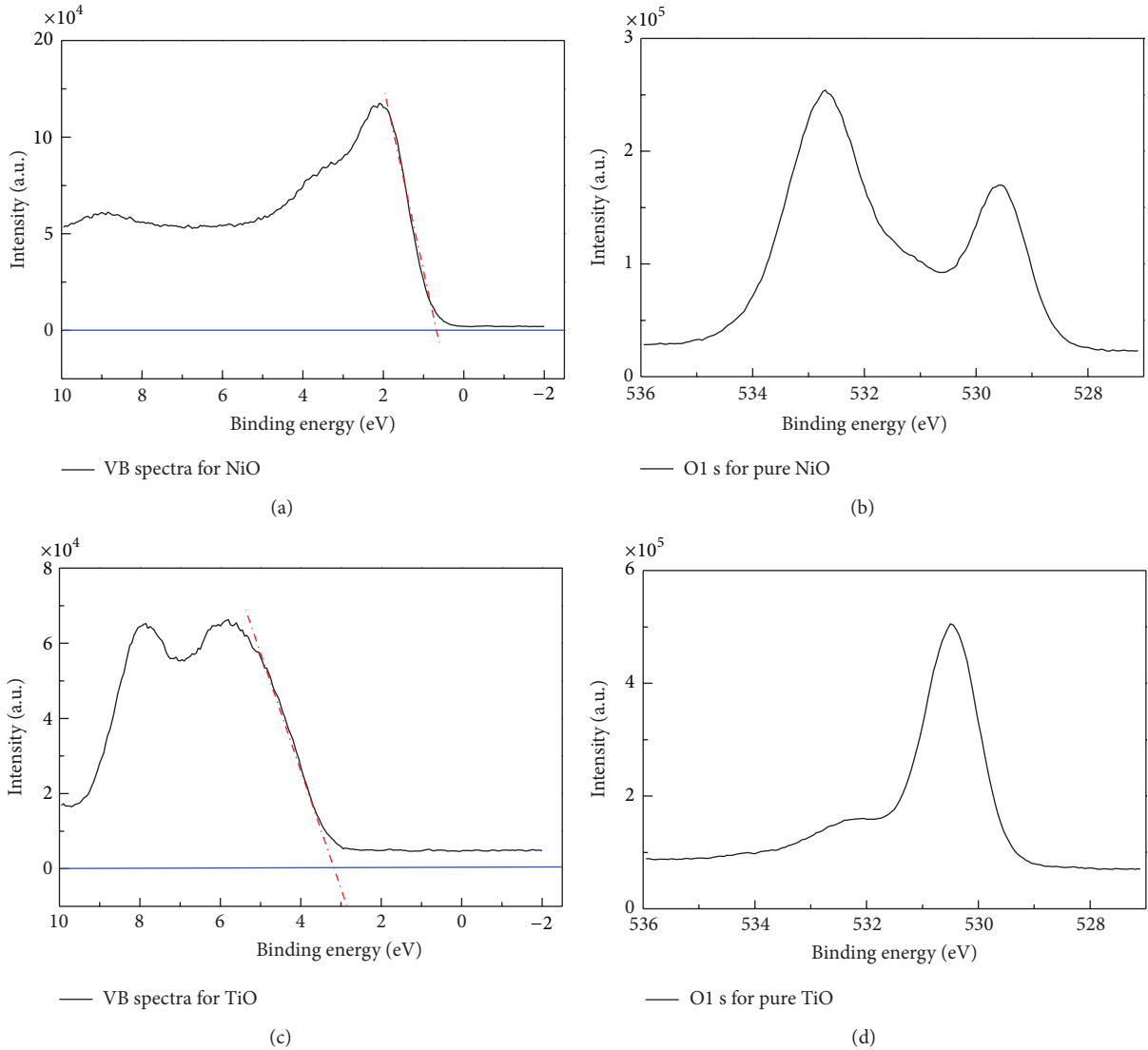
FIGURE 3: (a) VB spectrum of NiO, (b) VB spectrum of TiO$_2$, (c) O 1 s spectrum of NiO, and (d) O 1 s spectrum of TiO$_2$.

state [41–43]. Both measured both peaks are symmetric and the FWHM of Ti 2p 3/2 is found to be 1.1 eV that is matching with the reported values, and it is attributed to the defect free TiO$_2$ synthesized by sol-gel method (110) [42, 43]. The nickel 2p and Ti 2p peaks in the NiO/TiO$_2$ heterostructures are shown in Figures 2(c) and 2(d). It has been indicated that the measured peaks are symmetric relative to that of information obtained from the pure samples of NiO and TiO$_2$, the change in Ni 2p peak is observed from the value 0.3 eV to the binding energy value of 853.839 eV and the Ti 2p 3/2 is changed from the 0.056 to 459.16 eV. The valence-band (VB) spectrum of NiO and TiO$_2$ is shown in Figures 3(a) and 3(b). The valence-band maximum (VBM) value of 0.73 eV for NiO is extrapolated from the VB spectrum using linear fitting. The VB spectrum for TiO$_2$ was measured by similar a method as for NiO and is shown in Figure 3(b). and the VBM value of 0.73 eV was observed. For O 1 s in the NiO sample, the less intense peak at a binding energy of 529.47 eV corresponds

to the O 1 s peak of NiO. The very intense shoulder peak at 533.3 eV is assigned to the surface adsorbed oxygen as shown in Figure 3(c). The O 1 s spectrum of Ti–O is comprised on the two apparent peaks, one at 530.48 eV is attributed to the Ti–O bonds and the other at 532.21 eV because of the surface adsorbed species as shown in Figure 3(d). The reported method [44] was used for the measurement of valence-band offset of NiO/TiO$_2$ heterojunctions by applying the following formula:

$$\Delta E_V = \left(E_{\text{Ni 2p}}^{\text{NiO}} - E_{\text{VBM}}^{\text{NiO}} \right) - \left(E_{\text{Ti 2p}}^{\text{TiO}} - E_{\text{VBM}}^{\text{TiO}} \right) + \Delta E_{\text{CL}}. \quad (1)$$

Here $(E_{\text{Ni 2p}}^{\text{NiO}} - E_{\text{VBM}}^{\text{NiO}})$ is the energy difference between Ni 2p and VBM in the pure NiO nanostructures, $(E_{\text{Ti 2p}}^{\text{TiO}} - E_{\text{VBM}}^{\text{TiO}})$ is the energy difference between the Ti 2p and the VBM in the TiO$_2$, and $\Delta E_{\text{CL}} = (E_{\text{Ti 2p}}^{\text{TiO}} - E_{\text{Ni 2p}}^{\text{NiO}})$ is the energy difference between the Ti 2p and Ni 2p core levels (CLs) in the NiO/TiO$_2$
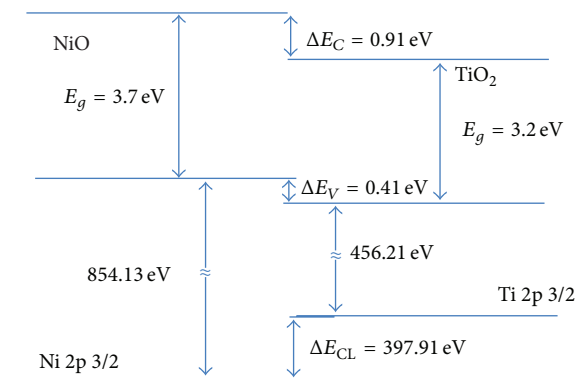
FIGURE 4: The schematic diagram of the band alignment.

heterostructures. Hence the measured valance-band offset of developed heterojunction is found to be ~0.41 eV. The conduction-band offset of NiO/TiO_2 heterojunction was measured by the following formula:

$$\Delta E_C = \left(E_{\text{band gap}}^{\text{TiO}} - E_{\text{band gap}}^{\text{NiO}} \right) - \Delta E_V. \tag{2}$$

The respective band gap for the NiO is 3.7 eV and 3.2 eV for TiO_2, respectively, at room temperature; thus the calculated ΔE_C is found to be ~0.91 eV. However the schematic diagram of the band alignment is depicted in Figure 4. It can be observed that a type-II band alignment is produced at the junction of NiO/TiO_2 heterojunction. The observed ratio of CBO and VBO $\Delta E_C/\Delta E_V$ is 2.21.

4. Conclusion

In this study, the hydrothermal approach was used for the development of p-type NiO/n-type TiO_2 heterojunction on the FTO glass substrate. The SEM and XRD techniques were used for the morphological and structural characterization. The XPS technique was used for the measurement of valence-band offset and the observed band offset was found to be ~0.41 eV and the conduction band of ~0.91 eV was determined. The ratio of conduction band and valence-band offset was found to be 2.21.

Conflict of Interests

The authors declare that there is no conflict of interests regarding the publication of this paper.

Acknowledgments

References

[1] G. R. Patzke, F. Krumeich, and R. Nesper, "Oxidic nanotubes and nanorods anisotropic modules for a future nanotechnology," *Angewandte Chemie—International Edition*, vol. 41, no. 14, pp. 2446–2461, 2002.

[2] M. Grätzel, "Sol-gel processed TiO_2 films for photovoltaic applications," *Journal of Sol-Gel Science and Technology*, vol. 22, no. 1-2, pp. 7–13, 2001.

[3] Z. X. Ge, A. X. Wei, J. Liu, W. Zhao, and C. B. Liu, "Synthesis and photovoltaic devices performance of single crystalline TiO_2 nanowire bundle arrays," *Journal of Inorganic Materials*, vol. 25, no. 10, pp. 1105–1109, 2010.

[4] H. Chen, W. Y. Fu, H. B. Yang et al., "Photosensitization of TiO_2 nanorods with CdS quantum dots for photovoltaic devices," *Electrochimica Acta*, vol. 56, no. 2, pp. 919–924, 2010.

[5] Y. K. Zhou, L. Cao, F. B. Zhang, B. L. He, and H. L. Li, "Lithium insertion into TiO_2 nanotube prepared by the hydrothermal process," *Journal of the Electrochemical Society*, vol. 150, no. 9, pp. A1246–A1249, 2003.

[6] P. Charoensirithavorn, Y. Ogomi, T. Sagawa, S. Hayase, and S. Yoshikawa, "A facile route to TiO_2 nanotube arrays for dye-sensitized solar cells," *Journal of Crystal Growth*, vol. 311, no. 3, pp. 757–759, 2009.

[7] M. Anpo, "Preparation, characterization, and reactivities of highly functional titanium oxide-based photocatalysts able to operate under UV-visible light irradiation: approaches in realizing high efficiency in the use of visible light," *Bulletin of the Chemical Society of Japan*, vol. 77, no. 8, pp. 1427–1442, 2004.

[8] B. Q. Su, Y. J. Ma, Y. L. Du, C. Yang, and C. M. Wang, "In situ photoelectrocatalytic degradation behavior of methylene blue on Nano-TiO_2 modified electrode," *Journal of the Electrochemical Society*, vol. 155, no. 10, pp. F213–F217, 2008.

[9] Y. Xie, "Photoelectrochemical application of nanotubular titania photoanode," *Electrochimica Acta*, vol. 51, no. 17, pp. 3399–3406, 2006.

[10] G. Yan, M. Zhang, J. Hou, and J. Yang, "Photoelectrochemical and photocatalytic properties of N+S co-doped TiO_2 nanotube array films under visible light irradiation," *Materials Chemistry and Physics*, vol. 129, no. 1-2, pp. 553–557, 2011.

[11] M. Zhang, J. Wu, J. Hou, and J. Yang, "Molybdenum and nitrogen co-doped titanium dioxide nanotube arrays with enhanced visible light photocatalytic activity," *Science of Advanced Materials*, vol. 5, no. 6, pp. 535–541, 2013.

[12] M. Zhang, J. Wu, D. Lu, and J. Yang, "Enhanced visible light photocatalytic activity for TiO_2 nanotube array films by codoping with tungsten and nitrogen," *International Journal of Photoenergy*, vol. 2013, Article ID 471674, 8 pages, 2013.

[13] R. Ciancio, E. Carlino, C. Aruta, D. MacCariello, F. M. Granozio, and U. S. Di Uccio, "Nanostructure of buried interface layers in TiO_2 anatase thin films grown on LaAlO3 and $SrTiO_3$ substrates," *Nanoscale*, vol. 4, no. 1, pp. 91–94, 2012.

[14] S. Guo, S. Han, H. Mao et al., "Synthesis and characterization of nitrogen and phosphate codoped titanium dioxide with excellent visible-light photocatalytic activity," *Journal of Alloys and Compounds*, vol. 544, pp. 50–54, 2012.

[15] I. Lee, J. B. Joo, Y. Yin, and F. Zaera, "A yolk@shell nanoarchitecture for Au/TiO_2 catalysts," *Angewandte Chemie—International Edition*, vol. 50, no. 43, pp. 10208–10211, 2011.

[16] Y. P. Guo, N. H. Lee, H. J. Oh et al., "Preparation of titanate nanotube thin film using hydrothermal method," *Thin Solid Films*, vol. 516, no. 23, pp. 8363–8371, 2008.

[17] C. Suwanchawalit and S. Wongnawa, "Triblock copolymer-templated synthesis of porous TiO_2 and its photocatalytic activity," *Journal of Nanoparticle Research*, vol. 12, no. 8, pp. 2895–2906, 2010.

[18] A. Michailowski, D. Almawlawi, G. S. Cheng, and M. Moskovits, "Highly regular anatase nanotubule arrays fabricated in porous anodic templates," *Chemical Physics Letters*, vol. 349, no. 1-2, pp. 1–5, 2001.

[19] Y. S. Tian, C. G. Hu, X. S. He, C. L. Cao, G. S. Huang, and K. Y. Zhang, "Titania nanotube arrays for light sensor and UV photometer," *Sensors and Actuators B*, vol. 144, no. 1, pp. 203–207, 2010.

[20] P. Xiao, D. Liu, B. B. Garcia, S. Sepehri, Y. Zhang, and G. Cao, "Electrochemical and photoelectrical properties of titania nanotube arrays annealed in different gases," *Sensors and Actuators B*, vol. 134, no. 2, pp. 367–372, 2008.

[21] W. Li, S. I. Shah, C. P. Huang, O. Jung, and C. Ni, "Metallorganic chemical vapor deposition and characterization of TiO_2 nanoparticles," *Materials Science and Engineering B*, vol. 96, no. 3, pp. 247–253, 2002.

[22] B. Mukherjee, C. Karthik, and N. Ravishankar, "Hybrid sol-gel combustion synthesis of nanoporous anatase," *Journal of Physical Chemistry C*, vol. 113, no. 42, pp. 18204–18211, 2009.

[23] K. Kanie and T. Sugimoto, "Shape control of anatase TiO_2 nanoparticles by amino acids in a gel-sol system," *Chemical Communications*, no. 14, pp. 1584–1585, 2004.

[24] H. Sato, T. Minami, S. Takata, and T. Yamada, "Transparent conducting p-type NiO thin films prepared by magnetron sputtering," *Thin Solid Films*, vol. 236, no. 1-2, pp. 27–31, 1993.

[25] X. C. Lou, X. J. Zhao, and X. He, "Boron doping effects in electrochromic properties of NiO films prepared by sol-gel," *Solar Energy*, vol. 83, no. 12, pp. 2103–2108, 2009.

[26] H. Steinebach, S. Kannan, L. Rieth, and F. Solzbacher, "H_2 gas sensor performance of NiO at high temperatures in gas mixtures," *Sensors and Actuators B*, vol. 151, no. 1, pp. 162–168, 2010.

[27] M. A. Abbasi, Z. H. Ibupoto, M. Hussain et al., "Potentiometric zinc ion sensor based on honeycomb-like NiO nanostructures," *Sensors*, vol. 12, no. 11, pp. 15424–15437, 2012.

[28] Z. Zhang, C. Shao, X. Li, C. Wang, M. Zhang, and Y. Liu, "Electrospun nanofibers of p-type NiO/n-type ZnO heterojunctions with enhanced photocatalytic activity," *ACS Applied Materials and Interfaces*, vol. 2, no. 10, pp. 2915–2923, 2010.

[29] C. Shifu, Z. Sujuan, L. Wei, and Z. Wei, "Preparation and activity evaluation of p-n junction photocatalyst NiO/TiO_2," *Journal of Hazardous Materials*, vol. 155, no. 1-2, pp. 320–326, 2008.

[30] Y. Ku, C. N. Lin, and W. M. Hou, "Characterization of coupled NiO/TiO_2 photocatalyst for the photocatalytic reduction of Cr(VI) in aqueous solution," *Journal of Molecular Catalysis A*, vol. 349, no. 1-2, pp. 20–27, 2011.

[31] Y. Chen, J. C. Crittenden, S. Hackney, L. Sutter, and D. W. Hand, "Preparation of a novel TiO_2-based p-n junction nanotube photocatalyst," *Environmental Science and Technology*, vol. 39, no. 5, pp. 1201–1208, 2005.

[32] J. L. Chung, J. C. Chen, and C. J. Tseng, "Preparation of TiO_2-doped ZnO films by radio frequency magnetron sputtering in ambient hydrogen-argon gas," *Applied Surface Science*, vol. 255, no. 5, pp. 2494–2499, 2008.

[33] J. K. Kang and S. W. Rhee, "Chemical vapor deposition of nickel oxide films from $Ni(C_5H_5)_2/O_2$," *Thin Solid Films*, vol. 391, no. 1, pp. 57–61, 2001.

[34] K. Zheng, L. Gu, D. Sun, X. Mo, and G. Chen, "The properties of ethanol gas sensor based on Ti doped ZnO nanotetrapods," *Materials Science and Engineering B*, vol. 166, no. 1, pp. 104–107, 2010.

[35] B. A. Reguig, A. Khelil, L. Cattin, M. Morsli, and J. C. Bernède, "Properties of NiO thin films deposited by intermittent spray pyrolysis process," *Applied Surface Science*, vol. 253, no. 9, pp. 4330–4334, 2007.

[36] R. G. S. Pala, W. Tang, M. M. Sushchikh et al., "CO oxidation by Ti- and Al-doped ZnO: oxygen activation by adsorption on the dopant," *Journal of Catalysis*, vol. 266, no. 1, pp. 50–58, 2009.

[37] R. Deng, B. Yao, Y. F. Li et al., "X-ray photoelectron spectroscopy measurement of n-ZnO/p-NiO heterostructure valence-band offset," *Applied Physics Letters*, vol. 94, no. 2, Article ID 022108, 2009.

[38] Y. Ishida, A. Fujimori, H. Ohta, M. Hirano, and H. Hosono, "Potential profiling of the nanometer-scale charge-depletion layer in n-ZnO/p-NiO junction using photoemission spectroscopy," *Applied Physics Letters*, vol. 89, no. 15, Article ID 153502, 2006.

[39] H. Long, G. J. Fang, H. H. Huang et al., "Ultraviolet electroluminescence from ZnO/NiO-based heterojunction light-emitting diodes," *Applied Physics Letters*, vol. 95, no. 1, Article ID 013509, 2009.

[40] P. Zurcher and R. S. Bauer, "Photoemission determination of dipole layer and VB−discontinuity formation during the MBE growth of GaAs on Ge(110)," *Journal of Vacuum Science and Technology A*, vol. 1, no. 2, pp. 695–700, 1982.

[41] W. Göpel, J. A. Anderson, D. Frankel et al., "Surface defects of $TiO_2(110)$: a combined XPS, XAES AND ELS study," *Surface Science*, vol. 139, no. 2-3, pp. 333–346, 1984.

[42] S. Pétigny, H. Mostéfa-Sba, B. Domenichini, E. Lesniewska, A. Steinbrunn, and S. Bourgeois, "Superficial defects induced by argon and oxygen bombardments on (110) TiO_2 surfaces," *Surface Science*, vol. 410, no. 2-3, pp. 250–257, 1998.

[43] S. A. Bilmes, P. Mandelbaum, F. Alvarez, and N. M. Victoria, "Surface and electronic structure of titanium dioxide photocatalysts," *Journal of Physical Chemistry B*, vol. 104, no. 42, pp. 9851–9858, 2000.

[44] S. H. Wei and A. Zunger, "Calculated natural band offsets of all II–VI and III–V semiconductors: chemical trends and the role of cation d orbitals," *Applied Physics Letters*, vol. 72, no. 16, pp. 2011–2013, 1998.